Chemical Geology 511 (2019) 256–264

Contents lists available at ScienceDirect

Chemical Geology

journal homepage: www.elsevier.com/locate/chemgeo

Cycles of trace elements and isotopes in the ocean – GEOTRACES and beyond

Plutonium in the western North Pacific: Transport along the Kuroshio and implication for the impact of Fukushima Daiichi Nuclear Power Plant accident☆

Junwen Wu[a,b], Minhan Dai[a,*], Yi Xu[a], Jian Zheng[c]

[a] State Key Laboratory of Marine Environmental Science, Xiamen University, Xiang'an District, Xiamen 361102, China
[b] College of Science, Shantou University, Shantou 515063, China
[c] Fukushima Project Headquarters, National Institute of Radiological Sciences, National Institutes for Quantum and Radiological Science and Technology, 491 Anagawa, Inage, Chiba 263-8555, Japan

ARTICLE INFO

Keywords:
Plutonium
Pacific Proving Grounds
Fukushima Daiichi Nuclear Power Plant accident
Western North Pacific
Kuroshio

ABSTRACT

This study examined Pu source terms in the western North Pacific (WNP) based on data collected in 2014 and 2015. The basin wide $^{240}Pu/^{239}Pu$ atom ratios ranged from 0.227 to 0.263 with an average value of 0.244 ± 0.011, consistently higher than that of global fallout (~0.180). The spatial distribution of $^{240}Pu/^{239}Pu$ atom ratios showed higher values within the Kuroshio region, the main western ocean boundary current, as compared to the zone off of the Kuroshio. There was also an overall decreasing trend of $^{240}Pu/^{239}Pu$ along the Kuroshio path to its extensions. $^{239+240}Pu$ activities in surface seawater exhibited a wide range from 1.15 to 4.30 mBq m^{-3} and their spatial distribution showed an increasing trend with latitude. Unlike the $^{240}Pu/^{239}Pu$ atom ratios, which had heavier isotopic compositions in the Kuroshio mainstream compared to the zone off of the Kuroshio, the $^{239+240}Pu$ activities were higher outside the Kuroshio than within the Kuroshio. These patterns in both Pu isotopic ratios and activities point towards a unique close-in fallout source, which levels down in its source term and has a high degree of scavenging during its transport along the Kuroshio, and can be traced back to a precursor, the North Equatorial Current, which originates near the Pacific Proving Grounds (PPG) with characteristically higher $^{240}Pu/^{239}Pu$ atom ratios. High $^{240}Pu/^{239}Pu$ atom ratios found in the zone outside the Kuroshio were transported from the Kuroshio via the formation and circulation of North Pacific Intermediate Water. We further revealed, using a simple two end-member mixing model, that the PPG source contributed 60 ± 13% of the Pu in the Kuroshio zone and 45 ± 10% in the zone off of the Kuroshio. Both the comparison of Pu isotopic composition in the WNP within a radius of 500 km or 1000 km off the Fukushima Daiichi Nuclear Power Plant (FDNPP) between prior to and post the accident and a simple first order mass balance calculation in terms of atmospheric deposition and release suggest that the Pu originating from the FDNPP accident, if any, was either negligible, or the input flux of $^{239+240}Pu$ was too small to significantly alter the Pu isotopic composition in the ambient seawater.

This article is part of a special issue entitled: "Cycles of trace elements and isotopes in the ocean – GEOTRACES and beyond" - edited by Tim M. Conway, Tristan Horner, Yves Plancherel, and Aridane G. González.

1. Introduction

The Fukushima Daiichi Nuclear Power Plant (FDNPP) accident occurred on March 11, 2011, released a large amount of highly volatile fission products (e.g., ^{131}I, ^{132}Te, ^{133}Xe, ^{134}Cs and ^{137}Cs) into the environment (Buesseler et al., 2017 and references therein). Over 80% of atmospheric fallout from FDNPP ultimately released into the ocean (Morino et al., 2011; Buesseler et al., 2011, 2017; Yoshida and Kanda, 2012; Kanda, 2013). To date, radioactive contamination from the FDNPP accident has been extensively investigated for the volatile fission products (Buesseler et al., 2011, 2012; Honda et al., 2012; Kanda, 2013; Kaeriyama et al., 2014), but only sparsely for the nonvolatile Pu isotopes.

The amount of $^{239+240}Pu$ released from the FDNPP accident is in the

☆ This article is part of a special issue entitled: "Cycles of trace elements and isotopes in the ocean – GEOTRACES and beyond" - edited by Tim M. Conway, Tristan Horner, Yves Plancherel, and Aridane G. González.

* Corresponding author.
E-mail address: mdai@xmu.edu.cn (M. Dai).

https://doi.org/10.1016/j.chemgeo.2018.12.006
Received 26 December 2017; Received in revised form 22 June 2018; Accepted 8 December 2018
Available online 13 December 2018

range of 1.0–3.5 × 10^9 Bq based on terrestrial and aerosol samples collected around the FDNPP site (Zheng et al., 2012, 2013; Schneider et al., 2013; Yamamoto et al., 2014; Shinonaga et al., 2014; Sakaguchi et al., 2014). Extremely high activity levels of Pu (~10^{-3} Bq mL^{-1}) were detected in the radioactive wastewater, such as the stagnant water in the basement of the reactor building and the concentrated water in the evaporation-concentration equipment, about six orders of magnitude higher than those in the ambient seawater of the western North Pacific (WNP) (METI, 2013). However, to the best of our knowledge, there are only very limited studies concerning the Pu isotopic composition of seawater in the WNP after the FDNPP accident. Sakaguchi et al. (2012) and Bu et al. (2014a) found no significant variation in the Pu isotopic composition ($^{239+240}$Pu activities: 2.15–5.59 mBq m^{-3}; ^{240}Pu/^{239}Pu atom ratios: 0.181–0.251) within 30–200 km of the FDNPP site before and after the FDNPP accident based on sampling conducted in 2011 and 2013. Even within 30 km off the FDNPP site, no significant Pu signature ($^{239+240}$Pu activities: 4.23–5.30 mBq m^{-3}; ^{240}Pu/^{239}Pu atom ratios: 0.221–0.242) was detectable from the FDNPP accident during a cruise in 2013 (37°–37.5° N, 141°–141.4° E) (Bu et al., 2015). Indeed, there was neither indication of any impacts from the FDNPP accident on the isotopic composition of the Pu along the coast of the Japanese archipelago ($^{239+240}$Pu activities: 2.4–9.5 mBq m^{-3}; ^{240}Pu/^{239}Pu atom ratios: 0.191–0.255) or in the subarctic region of the North Pacific Ocean (35–50° N, 140° E–130° W; $^{239+240}$Pu activities: 2.40–2.85 mBq m^{-3}; ^{240}Pu/^{239}Pu atom ratios: 0.18–0.20; ^{241}Pu/^{239}Pu atom ratios: 6 × 10^{-4}–9 × 10^{-4}) (Oikawa et al., 2015; Hain et al., 2017; Casacuberta et al., 2017). All these studies point towards no immediate impact of the Pu that was directly discharged into the ocean from the FDNPP. However, Pu released through atmospheric fallout has not been assessed in the WNP basin beyond the coast regions off Japan.

In assessing the basin wide impact of the FDNPP in terms of Pu, another close-in fallout Pu source is well known and should be considered: the Pacific Proving Grounds (PPG) in the Marshall Islands, located in the northern equatorial Pacific Ocean. This source term is characterized by ^{240}Pu/^{239}Pu atom ratios of 0.30–0.36 (Buesseler, 1997; Muramatsu et al., 2001), which are compared to the feature ratios of 0.30–0.38 from the FDNPP accident (Zheng et al., 2012; Schneider et al., 2013) but higher than the global fallout ratio of 0.180 ± 0.014 (Koide et al., 1985; Buesseler and Sholkovitz, 1987; Krey et al., 1976; Kelley et al., 1999). It is thought that the pathway of this Pu transport is via the North Equatorial Current (NEC), and subsequently the Kuroshio Current (Bowen et al., 1980). Over the last few decades, although PPG Pu signatures have indeed been observed in the WNP (Lee et al., 2004; Yamada et al., 2006; Yamada and Zheng, 2008; Zheng and Yamada, 2004, 2006) and in its marginal seas (Kim et al., 2004; Zheng and Yamada, 2005; Wang and Yamada, 2005; Liu et al., 2011; Wu et al., 2014, 2018), transport along the Kuroshio has not been fully examined or quantified.

Thus, our study sought to examine Pu source terms in the WNP, and determine whether there are any indications of the FDNPP's impact on the WNP basin beyond the coast regions off Japan. Notably, we sampled along the Kuroshio mainstream starting from the Luzon Strait to south of Japan. For comparison, the zone off of the Kuroshio was also sampled. Both the isotopic ratio and activity of Pu in the water column were determined to help elucidate Pu source functions and transport pathways, and to evaluate the impact of the FDNPP accident on the WNP basin.

2. Materials and methods

2.1. Study area

Unique oceanic circulation patterns exist in the WNP, making this region oceanographically complex. The NEC, which originates in the equatorial region, is a dominant circulation current in the tropical North Pacific Ocean. The westward flow of the NEC splits into two western boundary currents as it encounters the Philippine coast (Toole et al., 1990; Qu and Lukas, 2003). The northern branch forms the root of the Kuroshio and the southern branch becomes the Mindanao Current (Qu and Lukas, 2003). The Kuroshio flows northeastward along the boundary of both the South and East China Seas and the south and east coasts of Japan (Centurioni et al., 2004; Wang et al., 2011). The Kuroshio is known to be an important western boundary current, and plays a critical role in meridional mass and heat transport (Zhang et al., 2002) and in modulating the biogeochemistry and ecosystem dynamics in its adjacent marginal seas (e.g., Dai et al., 2013).

Before the FDNPP accident, Pu was deposited in the WNP mainly as a consequence of global fallout from atmospheric weapons testing in the late 1950s and early 1960s (Hirose et al., 1987; Povinec et al., 2004) and close-in fallout from the PPG in the Marshall Islands where above-ground nuclear weapons testing was carried out during the period 1946–1958 (Lee et al., 2004; Yamada et al., 2006; Yamada and Zheng, 2008; Zheng and Yamada, 2004, 2006). Therefore, the distribution of $^{239+240}$Pu activities showed considerable temporal and spatial variation; for example, $^{239+240}$Pu activities in WNP surface waters decreased exponentially from 10–50 mBq m^{-3} in the 1960s to 2.4–3.8 mBq m^{-3} during the 2000s (Povinec et al., 2004; Hirose et al., 2006), and $^{239+240}$Pu activities of surface seawater in the northern area of the Kuroshio were higher than those in the southern area of the Kuroshio (Povinec et al., 2004). Temporal changes in $^{239+240}$Pu activities are determined by the apparent residence time of Pu (12 ± 3 years), radioactive decay, and lateral and vertical removal processes (Hirose and Aoyama, 2003a; Povinec et al., 2005; Oikawa et al., 2015). Before the FDNPP accident, $^{239+240}$Pu activities in surface seawater were estimated to range from 1.0 to 2.5 mBq m^{-3} in the tropical and subtropical regions (south of the Kuroshio) and from 1.5 to 5.2 mBq m^{-3} in the transition area (north of the Kuroshio) (Hirose and Aoyama, 2003b). ^{240}Pu/^{239}Pu atom ratios from WNP surface seawater measured during the period 2000–2010 ranged from 0.199 to 0.246, with a mean value of 0.234 ± 0.025 (Lee et al., 2004; Yamada et al., 2006; Yamada and Zheng, 2008; Zheng and Yamada, 2004, 2006; Oikawa et al., 2015; Bu et al., 2015).

2.2. Sample collection

Nine samples were collected along the Kuroshio, and five additional samples from the outside the Kuroshio have been included for comparison. Samples were collected onboard the R/V *Kexue I* in the spring and winter of 2014 and onboard the R/V *Dongfanghong II* in the spring of 2015. The 2014 spring cruise is described elsewhere (Wu et al., 2018). To better represent the goals of this study, we renamed the stations in the Kuroshio mainstream zone Stns. K1–K9, and those off of the Kuroshio zone Stns. P1–P5 (Fig. 1). Basic sampling information is presented in Supporting Information (SI) Table S1. In the tropical region (10°–20° N), Stn. K1 was sampled in spring 2014, and Stns. K2, P1 and P2 were sampled in winter 2014. In the subtropical region (20°–35° N), Stns. K3–K5 were sampled in spring 2014, and Stns. K6–K9, P3 and P4 in spring 2015. Stn.P5 in the transition area (35°–40° N) was sampled in spring 2015. Two deep water samples at 200 and 500 m were collected at Stn. K8 in spring 2015 in Niskin bottles in a conductivity–temperature–depth (CTD) rosette system. The remaining samples were all collected from the surface using a built-in pumping system. Upon collection, an approximately 100 L unfiltered seawater sample was acidified with concentrated HNO_3 to a pH of ~1.6 for subsequent sample processing and Pu isotope measurements.

2.3. Sample processing and Pu isotope analysis

The sample processing and analytical procedures used for Pu isotopes are described in detail elsewhere (Bu et al., 2014a; Wu et al., 2018). In brief, a known amount of ^{242}Pu (IRMM–085, European Commission Joint Research Centre, Belgium) was added to the seawater

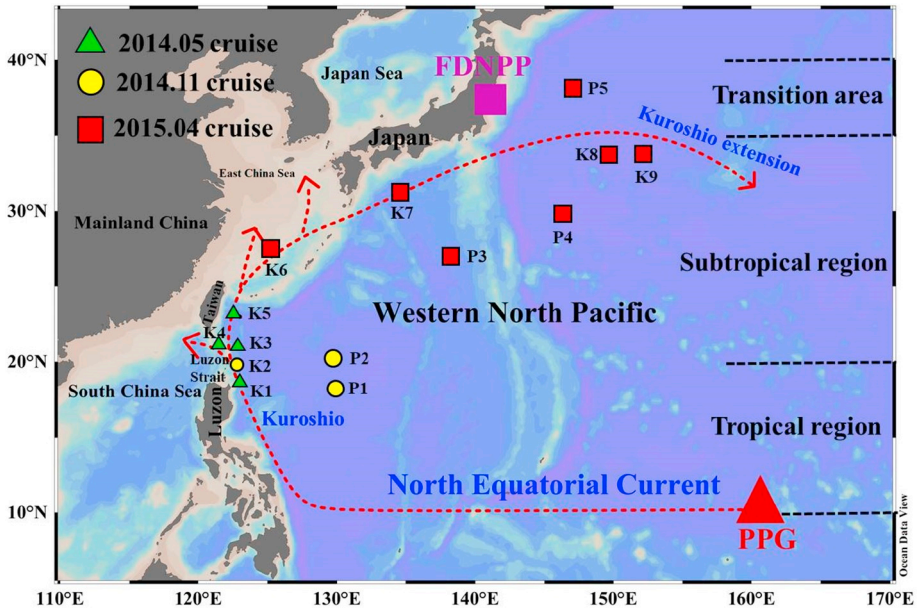

Fig. 1. Map of the western North Pacific Ocean showing a schematic chart of the North Equatorial Current-Kuroshio, and the location of the Pacific Proving Grounds (PPG) and Fukushima Daiichi Nuclear Power Plant (FDNPP). The PPG (red triangle) is located in the Marshall Islands and the FDNPP (pink square) is located in the Fukushima prefecture adjacent to the western North Pacific. The red dashed lines represent the North Equatorial Current and Kuroshio Current. Green triangles and yellow circles represent stations where seawater samples were collected in May and November 2014, respectively; and red squares represent stations where seawater samples were collected in April 2015. The water column was sampled at Stn. K8. (For interpretation of the references to color in this figure legend, the reader is referred to the web version of this article.)

samples as a yield determinant. The Pu in the spiked sample was co-precipitated with ferric hydroxide by adding ~10 mL of an Fe^{3+} solution (15.5 mg mL^{-1}) and adjusting the pH to ~9 with the addition of concentrated NH_4OH. The precipitate was then dissolved in 20 mL of 8 M HNO_3, and the valence state of Pu was adjusted to Pu^{4+} by adding $NaNO_2$. The Pu in the solution was subsequently purified with two-stage anion-exchange columns using AG 1–X8 and AG MP–1M (Bio-Rad) (Bu et al., 2014b; Wu et al., 2018). The final solution, evaporated to near dryness, was dissolved in 4% ultrapure HNO_3 (1.0 mL) and sent for MC–ICP–MS measurement (Nu Plasma HR, Nu Instruments Ltd., England) in the State Key Laboratory of Marine Environmental Science, Xiamen University. The instrument employed a DSN–100 high efficiency sample introduction system, containing a membrane desolvation unit and a conical concentric nebulizer. The recovery of Pu resulting from this procedure was 63.8 ± 5.6% (n = 42). The most significant interference in this method was usually caused by the formation of polyatomic uranium hydrides ($^{238}UH^+$) and peak tailing from the $^{238}U^+$ peak, resulting in an overestimation of the ^{239}Pu signal. The analytical method we employed in this study was able to effectively eliminate the U interferences by achieving an extremely high U decontamination factor of 6.0×10^7, which is comparable to previously reported values (3.0×10^7–1.0×10^8) (Bu et al., 2014a).

The data quality and the mass bias correction were assured by routine analyses of International Atomic Energy Agency (IAEA) certified reference material IAEA–443 (Irish Seawater). The measured $^{240}Pu/^{239}Pu$ atom ratio of this standard (0.230 ± 0.003, n = 16) was consistent with the verified value (0.229 ± 0.006). The analytical instrument was also tested by analyzing two additional reference materials: IAEA–385 (Irish Sea Sediment) and IAEA–384 (Fangataufa Lagoon Sediment). The measured $^{239+240}Pu$ activities and the $^{240}Pu/^{239}Pu$ atom ratios of these standards were in good agreement with the certified and previously reported values (Table S2). In addition, the operational blank count rates for ^{239}Pu and ^{240}Pu were assessed by measuring 100 L of pure water following the same chemical procedure for Pu determination in seawater. The limit of detection (LOD) was calculated based on the International Union of Pure and Applied Chemistry recommendations (Mocak et al., 1997). The LOD was calculated to be 0.44 fg mL^{-1} for ^{239}Pu and 0.36 fg mL^{-1} for ^{240}Pu, corresponding to 0.01 mBq m^{-3} for ^{239}Pu and 0.03 mBq m^{-3} for ^{240}Pu.

3. Results

For ease of presentation, we combined the datasets from the three cruises spanning two consecutive years (two in spring and one in winter), and assumed that the seasonal variation was minor. This assumption was based on the fact that the distribution of Pu in surface water is rather homogenous and that significant changes in Pu do not occur over timescales of 1–2 years, due to the long residence time of Pu in seawater and the long half-lives of its radioactive isotopes (Hirose and Aoyama, 2003a). Indeed, we observed that the difference in $^{240}Pu/^{239}Pu$ atom ratios at two adjacent stations, K1 sampled in spring 2014 and K2 sampled in winter 2014, was minor, < 2%, which is comparable to their relative standard deviations.

3.1. $^{240}Pu/^{239}Pu$ atom ratios

As shown in Table S1, $^{240}Pu/^{239}Pu$ atom ratios of surface seawater in the WNP during the investigated period ranged from 0.227 to 0.263, with an average value of 0.244 ± 0.011 (n = 14). Spatially, the $^{240}Pu/^{239}Pu$ atom ratios ranged from 0.243 to 0.263 (average = 0.253 ± 0.007, n = 7) in the Kuroshio mainstream zone and from 0.228 to 0.232 (average = 0.230 ± 0.003, n = 2) at the Kuroshio extension, showing a gradual decrease along the Kuroshio transport pathway from the Luzon Strait to south of Japan (Fig. S1). In contrast, the $^{240}Pu/^{239}Pu$ atom ratios outside the Kuroshio zone, 0.227–0.244 (average = 0.238 ± 0.007, n = 5), were lower than those of the Kuroshio mainstream. From the tropical region to the transition area, the distribution of $^{240}Pu/^{239}Pu$ atom ratios in the Kuroshio showed an overall decreasing trend with latitude (Fig. 2a), and the pattern of $^{240}Pu/^{239}Pu$ atom ratios in the zone off of the Kuroshio had no significant variation with latitude.

$^{240}Pu/^{239}Pu$ atom ratios in the water column at Stn. K8 varied from 0.227 to 0.249 (n = 3) in the upper 500 m (Table S1). These ratios were higher than those expected solely from global fallout (Kelley et al., 1999). The range of the $^{240}Pu/^{239}Pu$ atom ratios was comparable to that in the water column at Stn. F01 (36.5° N, 141.5° E, ~800 km away from Stn. K8) in the Western Pacific in October 2014 (0.23–0.27: Casacuberta et al., 2017). The depth profile of $^{240}Pu/^{239}Pu$ atom ratios at Stn. K8 showed a variation from 0.232 ± 0.006 at the surface to 0.227 ± 0.006 at 200 m, followed by a more gradual increase in values to 500 m, reaching 0.249. The vertical pattern of $^{240}Pu/^{239}Pu$ atom ratio was also consistent with that previously reported in the western Northwest Pacific Ocean (Fig. S2) (Yamada et al., 2007).

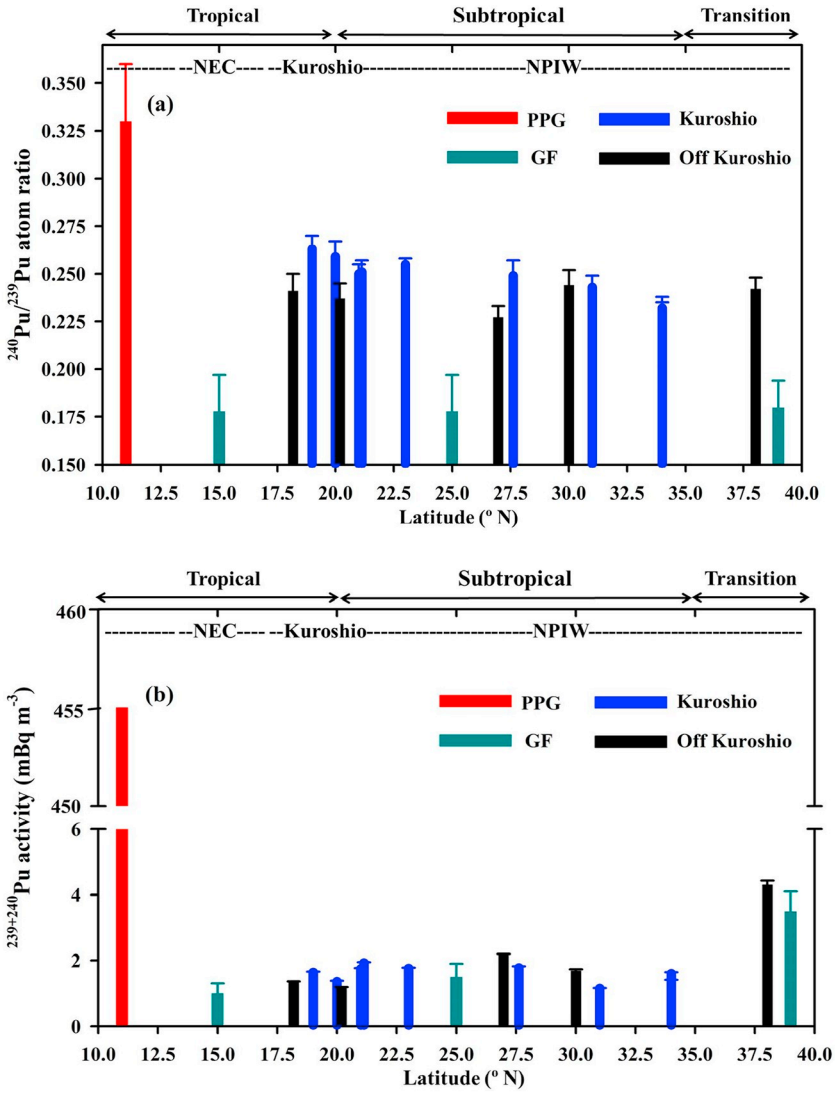

Fig. 2. Distribution of (a) ^{240}Pu/^{239}Pu atom ratios and (b) $^{239+240}$Pu activities in surface seawater as a function of latitude in the western North Pacific. PPG and GF represent Pacific Proving Grounds and Global Fallout. The Pu atom ratio of PPG and GF are taken from Buesseler (1997), Muramatsu et al. (2001) and Kelley et al. (1999). The activity of the PPG signal was obtained from the average values of Enewetak and Bikini lagoonal water collected in 2015 (Buesseler et al., 2018). The activities of GF are estimated based on data taken from Bowen et al. (1980) and Hirose and Aoyama (2003a, 2003b). North Equatorial Current (NEC)-Kuroshio Current and North Pacific Intermediate Water (NPIW) represent the main ocean current system in the corresponding latitudinal zone.

3.2. $^{239+240}$Pu activity

$^{239+240}$Pu activities of surface seawater in the WNP from 2014 to 2015 are listed in Table S1. They ranged from 1.15 to 4.30 mBq m^{-3}, with an average value of 1.79 ± 0.78 mBq m^{-3} (n = 14). The Kuroshio water $^{239+240}$Pu activities varied from 1.15 to 1.93 mBq m^{-3}, with an average value of 1.60 ± 0.25 mBq m^{-3} (n = 9). From the tropical region to the transition area, $^{239+240}$Pu activities within the Kuroshio showed no notable variation with respect to latitude, likely due to the fast transport of the Kuroshio. The travel time of Kuroshio water off the Luzon Strait starting from Stn. K1 to Stn. K9 was estimated as 66 days (42–155 days) under the assumption of a constant transport velocity (Centurioni et al., 2004). In contrast, $^{239+240}$Pu activities in water from the zone off of the Kuroshio were in a large range of 1.18–4.30 mBq m^{-3} (average = 2.13 ± 1.27 mBq m^{-3}, n = 5), showing a gradual increasing trend with latitude (Fig. 2b). For example, they increased from 1.26 mBq m^{-3} in the tropical region to 1.92 mBq m^{-3} in the subtropical region, followed by an increase to 4.30 mBq m^{-3} in the transition area. Meanwhile, we compiled all of the published data obtained in adjacent to Station P5 since the 2011 FDNPP accident, ranging from 1.97 to 5.59 mBq m^{-3} (n = 24) (Table S3: Sakaguchi et al., 2012; Bu et al., 2015; Hain et al., 2017; Casacuberta et al., 2017), which was comparable to our data at Station P5. Specifically, in August 2011, $^{239+240}$Pu activities in a distance of 450–500 km from the Station P5 were reported to be 5.23–5.50 mBq m^{-3} (n = 2) (Sakaguchi et al., 2012). In September 2012, $^{239+240}$Pu activities in a radius of 280 km off the Station P5 were in the range of 2.40–2.85 mBq m^{-3} (n = 2) (Hain et al., 2017). In a distance of 500 km off the Station P5, $^{239+240}$Pu activities of surface seawater collected in May 2013 and October 2014 were reported to be 4.23–5.30 mBq m^{-3} (n = 6: Bu et al., 2015) and 1.97–5.29 mBq m^{-3} (n = 14: Casacuberta et al., 2017), respectively. We incorporated these reported data and did a simple F-test and *t*-test in order to examine if $^{239+240}$Pu activities have a significant difference within and outside the Kuroshio (Lettner et al., 2000). As shown in Table S3, $^{239+240}$Pu activities (1.18–5.59 mBq m^{-3}, n = 29) outside the Kuroshio were statistically significantly higher than those (1.15–1.93 mBq m^{-3}, n = 9) within the Kuroshio (student *t*-test, $p < 0.05$).

$^{239+240}$Pu activities in the upper water column (0–500 m) at Stn. K8 varied from 1.61 to 5.38 mBq m^{-3} (n = 3) (Table S1), and gradually increased with the depth. Note that we were not entirely certain about the maximum Pu depth, owing to the coarse sampling resolution at depth. Nevertheless, the vertical distribution of $^{239+240}$Pu activities was consistent with typical Pu distribution patterns in the ocean, which show a gradual increase from the surface to the subsurface (Bowen et al., 1980; Tsumune et al., 2003). This pattern is also similar to that observed at Stn. F01, which is adjacent to Stn. K8, in October 2014 (Casacuberta et al., 2017) and the tropical eastern Pacific Ocean in 2003 (Kinoshita et al., 2011).

4. Discussion

4.1. Pu source and transport pathway

$^{240}Pu/^{239}Pu$ atom ratios (0.227–0.263) in WNP seawater, both at the surface and deeper in the water column, were all characteristically higher than those expected solely from global fallout (0.180 ± 0.014) (Kelley et al., 1999), implying that this area must have received Pu from the detonation of high-yield thermonuclear devices and/or fuel reactors at high burn-up; for example, the PPG and/or FDNPP accident. A heavier Pu isotopic ratio was observed in the Kuroshio mainstream zone as compared to the zone off of the Kuroshio, and its distribution was consistent with the transport pathway of the Kuroshio Current. Combined with the fact that $^{239+240}Pu$ activities within the Kuroshio were lower than those outside of the Kuroshio, this indicates that there was a decline in Pu source supply, and that Pu in the Kuroshio is readily scavenged. Most of Pu in the Kuroshio should be mainly from the PPG, which is released from sediments and seawater in contaminated lagoons. $^{239+240}Pu$ activities in PPG lagoonal seawater (455 mBq m^{-3}) and sediments (99 Bq kg^{-1}) remain several orders of magnitude higher than in the rest of the world's oceans, though slightly lower than the 1970s (Buesseler et al., 2018). It is estimated that $^{239+240}Pu$ from the PPG discharged into the North Pacific Ocean has an annual export flux of 0.26–0.73 TBq (1 TBq = 10^{12} Bq) (Buesseler et al., 2018). Nevertheless, these annual rates are orders of magnitude smaller than delivery rates via close-in fallout from the PPG in the 1950s (Buesseler et al., 2018). Lower $^{239+240}Pu$ activities in the Kuroshio must be related to the decrease in supply of Pu from the PPG over time. In addition, it is well known that the physical and/or chemical forms of Pu-bearing particles vary based on testing conditions (Buesseler, 1997). Close-in fallout from the PPG typically incorporates large quantities of partially and completely vaporized calcium, calcium oxides, calcium hydroxides and carbonates (typically > 1.0 μm in size) (Adams et al., 1960; Joseph et al., 1971). The Pu adhering to the relatively larger particles such as calcium hydroxides is by nature efficiently scavenged, and has a shorter residence time in seawater than Pu adhering to smaller particles. In contrast, global fallout particles are characterized by their sub-micron size (typically at 0.1–1.0 μm in size), as they originate directly from the vaporization and condensation of nuclear weapons materials (Adams et al., 1960; Joseph et al., 1971; Weimer and Langford, 1978). The Pu attached to these small particles is thus less efficiently scavenged, and has a longer residence time in seawater. In addition, it is known that the Kuroshio is characteristically elevated in diazotrophic activity which often stimulates diatom growth and increases export efficiency (Kitajima et al., 2009; Shiozaki et al., 2010; Bonnet et al., 2016). Indeed, the nitrogen fixer-*Trichodesmium* flourishes in the Kuroshio and its abundances were found to be positively correlated with diatom cells > 10 μm in diameter ($p < 0.05$) (Chen et al., 2008, 2011). Diatom vertical distributions also showed a maximum abundance at the surface, which coincided with the highest cell densities of *Trichodesmium* (Chen et al., 2011). In contrast to the Kuroshio, the zone outside the Kuroshio is sparsely inhabited by *Trichodesmium* and showed no surface maxima in the vertical distributions of *Trichodesmium* or diatom abundance (Kitajima et al., 2009; Chen et al., 2011). This indicated the Kuroshio potentially has a higher export efficiency compared to the zone off of the Kuroshio, despite the fact that particle abundances in these two regimes are not significantly different (Nakajima, 1973). Therefore, we suggested that the lower $^{239+240}Pu$ activity of the Kuroshio was linked primarily to the decrease in PPG supply over time, coinciding with high degrees of scavenging during transport along the Kuroshio.

These insights imply that the high $^{240}Pu/^{239}Pu$ atom ratios in the Kuroshio could be traced back to their precursor, the NEC, which originates approximately from the PPG. The Enewetak and Bikini Atolls are located within the NEC, and large–scale US nuclear tests conducted at these sites in the 1950s released a substantial radioactive fallout yield (Bowen et al., 1980; Buesseler, 1997) which might have been transported westward by the NEC and subsequently fed into its northward bifurcation, the Kuroshio Current off the Philippines. This high $^{240}Pu/^{239}Pu$ "stream" along the NEC–Kuroshio was evident when compared with $^{240}Pu/^{239}Pu$ atom ratios beyond this pathway in the WNP (0.207 ± 0.010, n = 4) (Yamada et al., 2006) and its adjacent marginal seas, such as in the China Sea (0.236 ± 0.017, n = 21: Yamada and Zheng, 2011; Wu et al., 2018), the Sulu and Indonesian Seas (0.237 ± 0.007, n = 4: Yamada et al., 2006), and the Japan Sea (0.240 ± 0.010, n = 24: Kang et al., 1997; Hirose et al., 1999, 2002; Yamada and Zheng, 2008). The supply of Pu from the PPG via the NEC-Kuroshio into the WNP appears to be continuous, as evident from the persistently high $^{240}Pu/^{239}Pu$ atom ratios observed in the WNP at present, some 60–70 years since US nuclear weapons testing was banned on the Marshall Islands.

High $^{240}Pu/^{239}Pu$ atom ratios of samples from outside the Kuroshio zone (average = 0.238 ± 0.007) may be linked to the formation and circulation of North Pacific Intermediate Water (NPIW), which is a prominent feature of the entire North Pacific subtropical gyre and is well-defined as the salinity minimum at depths of 300–1000 m (Yasuda et al., 1996; Talley, 1997; Hansell et al., 2002). Newly formed NPIW is a mixture of recently ventilated, relatively fresh Oyashio water (~45%), and older, more saline Kuroshio water (~55%) of a similar density (Yasuda et al., 1996; Talley, 1997). Mixing between these water masses and the formation of new NPIW water occurs to the east of Japan, where stations Stns. K8 and K9 were located (Talley, 1997). This mixed water region is located in the inter-frontal zone between the Oyashio Front and the Kuroshio extension (Yasuda et al., 1996). Kumamoto et al. (2014) further describe the formation and circulation of the NPIW, including formation areas and the subduction of North Pacific Subtropical Mode Water (STMW) and Central Mode Water (CMW). In the subtropical region (20°–35° N), higher $^{240}Pu/^{239}Pu$ atom ratios in the Kuroshio could be transported to the zone off of the Kuroshio by the spreading and subduction of STMW. For example, to the south of the Kuroshio extension between about 30° and 35° N, STMW is formed and penetrates to a depth of about 300–500 m (Kumamoto et al., 2014). Subsequently, STMW spreads to near the subtropical front (Aoyama et al., 2006) through advection over the Kuroshio recirculation region (Suga and Hanawa, 1990, 1995). Other studies also illustrate the spreading and subduction of STMW in the subtropical region: in June 2012, ^{134}Cs activity reached a maximum of 6.12 ± 0.50 Bq m^{-3} at a depth of 151–m at 29° N, 165° E (Aoyama et al., 2016); and Kumamoto et al. (2014) found that the subsurface maximum in ^{134}Cs activity observed along 149° E is associated with the formation and subduction of STMW. Indeed, at Stn. K8, which is located in the formation area of STMW, the predominant temperature (16.4–17.7 °C), salinity (34.68–34.76) and potential density (σ_θ: 25.0–25.6) ranges were similar to those of STMW (Oka, 2009; Kumamoto et al., 2014). ^{137}Cs activity in the upper 500 m at Stn. K8 showed a gradual increase with depth, ranging from 2.28–2.83 Bq m^{-3}, further suggesting the subduction of STMW. In the tropical region between 10° and 20° N, high Pu isotopic ratios outside the Kuroshio zone (i.e., Stns. P1 and P2) were potentially caused by the spreading of CMW. The formation area of CMW is located in the transition area in the central North Pacific (Suga et al., 1997). CMW spreads generally eastward along the North Pacific Current, turns southward and then westward (Kumamoto et al., 2014). Aoyama et al. (2016) also show that high ^{134}Cs activity derived from the FDNPP accident in the transition area is introduced into the ocean's interior on a 1-year time scale through CMW formation and subduction.

4.2. Comparisons with data prior to the FDNPP accident

Our $^{240}Pu/^{239}Pu$ atom ratios measured after the FDNPP accident were compared to background isotopic data obtained from prior to the accident in the WNP (average = 0.234 ± 0.025) (Lee et al., 2004; Yamada et al., 2006; Yamada and Zheng, 2008; Zheng and Yamada,

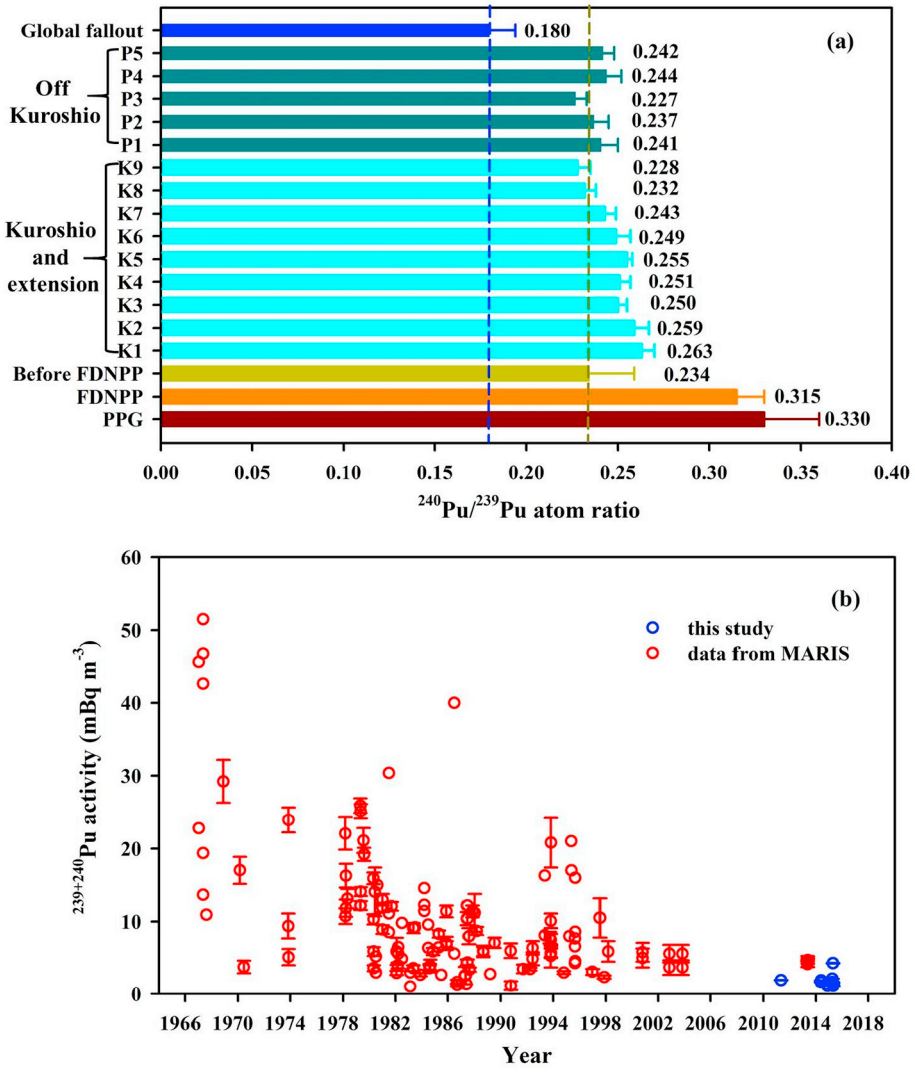

Fig. 3. Comparison of $^{240}Pu/^{239}Pu$ atom ratios with historical data (a); and the temporal variation of $^{239+240}Pu$ activity in surface seawater of the western North Pacific (15–40° N, 110–160° E) (b). Blue and dark yellow dashed lines (a) represent the Pu atom ratio of global fallout and pre-FDNPP accident data in the WNP. Blue and red circles (b) represent data from this study and historical data from MARIS (Marine Information System, International Atomic Energy Agency: https://maris.iaea.org/Home.aspx). (For interpretation of the references to color in this figure legend, the reader is referred to the web version of this article.)

2004, 2006). Specifically, the $^{240}Pu/^{239}Pu$ atom ratios in the Kuroshio (average = 0.253 ± 0.007) were comparable to the reported values in the Kuroshio and Kuroshio recirculation region before the FDNPP accident (Kim et al., 2004; Hirose et al., 2006), and the $^{240}Pu/^{239}Pu$ atom ratios in the zone off of the Kuroshio (average = 0.238 ± 0.007) were also comparable to before the FDNPP accident (Fig. 3a). It was thus difficult to determine whether there were any Pu signals from the FDNPP, due to its similarity to the PPG in terms of $^{240}Pu/^{239}Pu$ atom ratios; i.e., 0.30–0.36 for the PPG (Buesseler, 1997; Muramatsu et al., 2001) and 0.30–0.38 for the FDNPP accident (Zheng et al., 2012; Schneider et al., 2013). In addition, we estimated the input of FDNPP $^{239+240}Pu$ at four chosen stations (Stns. K7–K9 within the Kuroshio and Stn. P5 outside the Kuroshio) within 1000 km radius off the FDNPP and compared $^{240}Pu/^{239}Pu$ atom ratios and $^{239+240}Pu$ activities with background data obtained from adjacent stations prior to the FDNPP accident. Using an atmospheric deposition model, taking Pu activity of 130 nBq/m^3 in aerosols at a distance of 120 km off the FDNPP (Shinonaga et al., 2014) and adopting the upper limit of the deposition parameters (υ_d–dry deposition velocity (1.8 cm s^{-1}): McMahon and Denison, 1979; Duce et al., 1991; Giardina and Buffa, 2018; *P*–precipitation (300 mm/month): Giambelluca et al., 2013; *S*–the scavenging ratio in wet deposition (2000 g m^{-3}) and ρ_0–the density of atmosphere (1200 g m^{-3}): Duce et al., 1991), we calculated the maximal Pu deposition flux as 0.20 mBq m^{-2} day^{-1}, which is one order of magnitude higher than that in Tsukuba, Japan prior to the FDNPP accident (Hirose et al., 2003). Such input would result in a new Pu activity of surface seawater (upper 10 m) at the four chosen stations to be < 0.02 mBq m^{-3}, which is comparable to the measurement uncertainty of Pu. We point out that this estimation is subject to large uncertainty but they represent the maximal estimation. Moreover, we compared the $^{239+240}Pu$ activities and $^{240}Pu/^{239}Pu$ atom ratios of surface water at the four chosen stations with background data obtained from adjacent stations prior to the FDNPP accident. As shown in Table S4, within the Kuroshio, $^{239+240}Pu$ activity (1.15 ± 0.01 mBq m^{-3}) at Station K7 was comparable to the background value (1.5 ± 0.4 mBq m^{-3}) prior to the FDNPP accident collected in a distance of ~160 km off the Station K7 (Hirose et al., 2001). $^{239+240}Pu$ activities (1.40–1.61 mBq m^{-3}) and $^{240}Pu/^{239}Pu$ atom ratios (0.228–0.232) at Stations K8–K9 were comparable to those reported prior to the FDNPP accident in a distance of 600 km off the Stations K8–K9 (1.68 ± 0.28 mBq m^{-3} and 0.225 ± 0.037: Norisuye et al., 2006). Outside the Kuroshio, $^{239+240}Pu$ activities and $^{240}Pu/^{239}Pu$ atom ratios (4.30 ± 0.13 mBq m^{-3} and 0.242 ± 0.006) at Station P5 were comparable to the reported values (4.13 ± 0.63 mBq m^{-3} and

0.231 ± 0.035) prior to the FDNPP accident obtained in a radius of 500 km off the Station P5 (Oikawa et al., 2015). Therefore, we did not observe changes in Pu isotopic composition at Stns. K7–K9 and P5 post the FDNPP accident as compared to the reported data obtained from the adjacent stations prior to the FDNPP accident (Hirose et al., 2001; Norisuye et al., 2006; Oikawa et al., 2015). Such comparison suggests that the input of $^{239+240}$Pu from the FDNPP accident would not alter the Pu isotopic composition in the radius of 500 km or 1000 km off the FDNPP.

We could also assess the impact of the Pu released from the FDNPP. The amount of $^{239+240}$Pu released from the FDNPP accident is reported to be 1.0–3.5 × 10^9 Bq (Zheng et al., 2012, 2013; Schneider et al., 2013; Yamamoto et al., 2014; Shinonaga et al., 2014; Sakaguchi et al., 2014). Assuming Pu behaviors similarly to Cs and 80% of the atmospheric Cs released deposited in the ocean (Buesseler et al., 2017), we estimate the maximum Pu released into ocean via atmospheric deposition is 0.8–2.8 × 10^9 Bq. Assuming that weapon tests derived $^{239+240}$Pu in the North Pacific is 3.6 PBq (calculated from ^{137}Cs: Buesseler, 2014; and considering a $^{239+240}$Pu/^{137}Cs activity ratio of 1.2%: Povinec et al., 2005), the new Pu derived from FDNPP would account for < 0.0001% of the weapon tests derived $^{239+240}$Pu in the North Pacific Ocean. In summary, both the comparison of Pu isotopic composition in the WNP within a radius of 500 km or 1000 km off the FDNPP between prior to and post the accident and a simple first order mass balance calculation in terms of atmospheric deposition and release suggest the input of FDNPP $^{239+240}$Pu would not alter the Pu isotopic composition. On the other hand, a heavier Pu isotopic ratio was observed in the Kuroshio mainstream zone as compared to the zone off of the Kuroshio, and its distribution was consistent with the transport pathway of the Kuroshio Current. We also confirmed that the higher ^{240}Pu/^{239}Pu atom ratios in the Kuroshio could be traced back to their precursor, the NEC, which originates approximately from the PPG in the above discussion. These insights imply that Pu from the PPG was still a dominant source.

$^{239+240}$Pu activity in WNP surface seawater was almost identical before and after the FDNPP accident. In the tropical region, $^{239+240}$Pu activities (1.38 ± 0.19 mBq m^{-3}, n = 4) were comparable to those reported for 1996 in an area adjacent to our study area (1.54 ± 0.04 mBq m^{-3}, n = 2) (Yamada et al., 2006). In the subtropical region, $^{239+240}$Pu activities (1.69 ± 0.29 mBq m^{-3}, n = 9) were slightly lower than those reported for the period 1991–2000 in an area adjacent to our study area (1.7–6.2 mBq m^{-3}) (Yamada et al., 2006; Povinec et al., 2004). In addition, these $^{239+240}$Pu activity levels were also lower than those of the adjacent marginal seas, such as in the SCS from 2012 to 2014 (2.34 ± 0.38 mBq m^{-3}, n = 18) (Wu et al., 2018) and the Japan Sea from 1984 to 1997 (3–25 mBq m^{-3}) (Hirose et al., 2002; Yamada and Zheng, 2008). In the transition area, high $^{239+240}$Pu activity at Stn. P5 was also comparable to reported results from the coastal area adjacent to the FDNPP site (within the 0–200 km zone) (4.15 ± 0.35 mBq m^{-3}, n = 5) during 2013 (Bu et al., 2014a, 2015) and the background value before the FDNPP (1.5–5.2 mBq m^{-3}) (Povinec et al., 2005; Oikawa et al., 2015; Bu et al., 2015). In addition, we made another comprehensive comparison with long-term data over the past sixty years, made publicly available by the Marine Information System (MARIS, geographical restriction: 15°–40° N, 110°–160° E; maintained by the IAEA: https://maris.iaea.org/Home.aspx) (Fig. 3b). As Fig. 3b shows, $^{239+240}$Pu activity levels of surface seawater in the WNP decreased exponentially from 50 to 2 mBq m^{-3} from 1960 to 2010. Our measured results were almost identical to the 2010 pre-FDNPP accident value. Taken together, we suggested Pu contributed from the FDNPP accident, if any, to the WNP basin was negligible. The spatial distribution of $^{239+240}$Pu activity showed an increase from the tropical region to the transition area, possibly related to the latitudinal distribution of $^{239+240}$Pu deposition; i.e., high fluxes occur at mid-latitudes and low fluxes occur at low-latitudes (Bowen et al., 1980; Hirose et al., 2001).

In summary, both the comparison of Pu isotopic composition in the WNP within a radius of 500 km or 1000 km off the FDNPP between prior to and post the accident and a simple first order mass balance calculation in terms of atmospheric deposition and release suggest there were no indications of the FDNPP's impact on the WNP basin. The pathway of Pu transported from the PPG into the WNP was primarily via the NEC-Kuroshio Current and the spreading and subduction of NPIW, including both STMW and CMW. The Pu isotopes in the seawater of the Kuroshio mainstream zone were characterized by high ^{240}Pu/^{239}Pu atom ratios and low $^{239+240}$Pu activities compared to those measured in the zone off of the Kuroshio.

4.3. Quantitative estimation of the PPG Pu contribution

While the PPG is a continuous Pu source term to the WNP, other possible sources, such as the Chernobyl nuclear accident, on-going nuclear power plants along the coast of the study area and other local fallouts, are excluded (Kim et al., 2004; Wu et al., 2018). Our measured data in the WNP also fell well within the characteristic values of global fallout and close-in fallout from the PPG, with the PPG as the dominant source to the WNP. Therefore, we can state that the Pu in the WNP was sourced from both global fallout and close-in fallout from the PPG. We can then estimate the relative contribution of the PPG to Pu in the WNP using a two end-member mixing model (Krey, 1976; Wu et al., 2014, 2018):

$$Y = \frac{(Pu)_P}{(Pu)_G} = \frac{(R_G - R_S)(1 + 3.674R_P)}{(R_S - R_P)(1 + 3.674R_G)} \quad (1)$$

where (Pu) and R represent the $^{239+240}$Pu activity and the ^{240}Pu/^{239}Pu atom ratio; the subscripts P, G and S refer to the PPG, global fallout and the WNP; and the coefficient 3.674 is a factor used to convert between the activity ratio and atom ratio of ^{240}Pu/^{239}Pu. In the calculation, R_G was taken to be 0.180 ± 0.014 (Kelley et al., 1999) and R_P was 0.330 ± 0.030 (Buesseler, 1997; Muramatsu et al., 2001). Pu in the WNP derived from the PPG was calculated to be on average 52 ± 12%. This estimate is slightly higher than previous ones made for the SCS (~42%: Yamada et al., 2006; Wu et al., 2018) and the Sulu Sea (~39%: Yamada et al., 2006), indicating that Pu from the PPG is more readily scavenged in the marginal seas as compared to the WNP, due to elevated biological productivity and particle abundance (Han et al., 2012). However, our estimate of PPG Pu contribution is slightly lower than estimates made in sediments of the northern SCS shelf (~68%: Wu et al., 2014) and the SCS basin (~57%: Dong et al., 2010), further indicating that the close-in fallout Pu from the PPG was more readily scavenged from the surface water than was Pu derived from global fallout, and preferentially accumulated in sediments (Buesseler, 1997; Wu et al., 2018). In addition, the PPG contribution to the WNP showed a gradual decrease along the northeastward transport pathway of the Kuroshio. Finally, the PPG contribution of Pu to the Kuroshio zone was ~30% higher than outside of the Kuroshio zone, with estimated contributions of 60 ± 13% for the Kuroshio mainstream zone and 45 ± 10% for the zone off of the Kuroshio.

5. Conclusions

High ^{240}Pu/^{239}Pu atom ratios (0.227–0.263) were observed in both surface waters and at depth during 2014–2015, indicating non-global fallout Pu sources to the WNP. The spatial distribution of ^{240}Pu/^{239}Pu atom ratios showed higher ratios within the Kuroshio region as compared to the zone off of the Kuroshio. There was also an overall decreasing trend in ratios along the Kuroshio pathway to its extension areas. $^{239+240}$Pu activities in WNP surface seawater ranged from 1.15 to 4.30 mBq m^{-3}, showing an increase with latitude. We confirmed the presence of the non-global fallout Pu signature from the PPG by comparing ^{240}Pu/^{239}Pu atom ratios and $^{239+240}$Pu activities between the zones within and outside the Kuroshio. Higher ^{240}Pu/^{239}Pu atom ratios in the Kuroshio were mainly from the PPG, transported via the NEC–Kuroshio Current, although high Pu isotopic ratios also found in the zone off of the Kuroshio were initially

derived from the Kuroshio via the formation and circulation of NPIW, including STMW and CMW. We further revealed, using a simple two end-member mixing model, that this PPG source contributed 60 ± 13% of the Pu in the Kuroshio zone and 45 ± 10% of the Pu in the zone off of the Kuroshio. Additionally, Pu seawater isotopes in the Kuroshio mainstream zone were featured by high $^{240}Pu/^{239}Pu$ atom ratios and low $^{239+240}Pu$ activities compared to the zone off of the Kuroshio. Both the comparison of Pu isotopic composition in the WNP within a radius of 500 km or 1000 km off the FDNPP between prior to and post the accident and a simple first order mass balance calculation in terms of atmospheric deposition and release suggest that the Pu originating from the FDNPP accident, if any, was either negligible, or the input flux of $^{239+240}Pu$ was too small to significantly alter the Pu isotopic composition in the ambient seawater. Finally, from the determination of Pu isotopic ratios and activity levels in the WNP basin, we have established a baseline for future environmental risk assessment in this region.

Notes

The authors declare no competing financial interest.

Author contributions

The manuscript was written through contributions of all the authors. All authors have given approval to the final version of the manuscript.

Acknowledgements

This work was supported by the Major National Scientific Research Project (2015CB954000), STU Scientific Research Foundation for Talents (NTF18011), the JSPS KAKENHI (JP17k00537), and partly supported by the Grant of Fukushima Prefecture related to Research and Development in Radiological Sciences. The authors express their gratitude to Shuimiao Lu for providing assistance in sample measurements. The authors are also grateful to the crew of the *Dongfanghong II* and *Kexue I* for providing much help during the cruises. Professor John Hodgkiss is thanked for his help with English. Three anonymous reviewers are thanked for their constructive comments and suggestions that have contributed to improve this paper.

Appendix A. Supplementary material

Supporting information to this article can be found online at https://doi.org/10.1016/j.chemgeo.2018.12.006.

References

Adams, C.E., Farlow, N.H., Schell, W.R., 1960. The compositions, structures and origins of radioactive fallout particles. Geochim. Cosmochim. Acta 18, 42–56.
Aoyama, M., Hirose, K., Igarashi, Y., 2006. Re-construction and updating our understanding on the global weapons test ^{137}Cs fallout. J. Environ. Monit. 8, 431–438.
Aoyama, M., Hamajima, Y., Hult, M., Uematsu, M., Oka, E., Tsumune, D., Kumanoto, Y., 2016. ^{134}Cs and ^{137}Cs in the North Pacific Ocean derived from the March 2011 TEPCO Fukushima Dai-ichi nuclear power plant accident, Japan. Part one: surface pathway and vertical distributions. J. Oceanogr. 72, 53–65.
Bonnet, S., Berthelot, H., Kubo, K.T., Fawcett, S., Rahav, E., L'Helguen, S., Frank, I.B., 2016. Dynamics of N_2 fixation and fate of diazotroph-derived nitrogen in a low-nutrient, low-chlorophyll ecosystem: results from the VAHINE mesocosm experiment (New Caledonia). Biogeosciences 13, 2653–2673.
Bowen, V.T., Noshkin, V.E., Livingston, H.D., Volchok, H.L., 1980. Fallout radionuclides in the Pacific Ocean: vertical and horizontal distribution, largely from GEOSESC station. Earth Planet. Sci. Lett. 49, 411–434.
Bu, W.T., Zheng, J., Guo, Q.J., Aono, T., Tagami, K., Uchida, S., Tazoe, H., Yamada, M., 2014a. Ultra-trace plutonium determination in small volume seawater by sector field inductively coupled plasma mass spectrometry with application to Fukushima seawater samples. J. Chromatogr. A 1337, 171–178.
Bu, W.T., Zheng, J., Guo, Q.J., Aono, T., Tazoe, H., Tagami, K., 2014b. A method of measurement of ^{239}Pu, ^{240}Pu, ^{241}Pu in high U content marine sediments by sector field ICP-MS and its application to Fukushima sediment samples. Environ. Sci. Technol. 48, 534–541.
Bu, W.T., Zheng, J., Aono, T., Wu, J.W., Tagami, K., Uchida, S., Guo, Q.J., Yamada, M., 2015. Pu distribution in seawater in the near coastal area off Fukushima after the Fukushima Daiichi Nuclear Power Plant accident. J. Nucl. Radiochem. Sci. 15, 1–6.
Buesseler, K.O., 1997. The isotopic signature of fallout plutonium in the North Pacific. J. Environ. Radioact. 36, 69–83.
Buesseler, K.O., 2014. Fukushima and ocean radioactivity. Oceanography 27, 92–105.
Buesseler, K.O., Sholkovitz, E.R., 1987. The geochemistry of fallout Pu in the north Atlantic: II. $^{240}Pu/^{239}Pu$ ratios and their significance. Geochim. Cosmochim. Acta 51, 2623–2637.
Buesseler, K.O., Aoyama, M., Fukasawa, M., 2011. Impacts of the Fukushima nuclear power plants on marine radioactivity. Environ. Sci. Technol. 45, 9931–9935.
Buesseler, K.O., Jayne, S.R., Fisher, N.S., Rypina, I.I., Baumann, H., Baumann, Z., Breier, C.F., Douglass, E.M., George, J., Macdonald, A.M., Miyamoto, H., Nishikawa, J., Pike, S.M., Yoshida, S., 2012. Fukushima-derived radionuclides in the ocean and biota off Japan. Proc. Natl. Acad. Sci. 109, 5984–5988.
Buesseler, K.O., Dai, M.H., Aoyama, M., Benitez-Nelson, C., Charmasson, S., Higley, K., Maderich, V., Masque, P., Morris, P.J., Oughton, D., Smith, J.N., 2017. Fukushima Daiichi-derived radionuclides in the ocean: transport, fate and impacts. Annu. Rev. Mar. Sci. 9, 173–203.
Buesseler, K.O., Charette, M.A., Pike, S.M., Henderson, P.B., Kipp, L.E., 2018. Lingering radioactivity at the Bikini and Enewetak Atolls. Sci. Total Environ. 621, 1185–1198.
Casacuberta, N., Christl, M., Buesseler, K.O., Lau, Y.S., Vockenhuber, C., Castrillejo, M., Synal, H.A., Masque, P., 2017. Potential release of ^{129}I, ^{236}U, and Pu isotopes from the Fukushima Dai-ichi nuclear power plants to the ocean from 2013 to 2015. Environ. Sci. Technol. 51, 9826–9835.
Centurioni, L.R., Niiler, P.P., Lee, D.K., 2004. Observations of inflow of Philippine Sea surface water into the South China Sea through the Luzon Strait. J. Phys. Oceanogr. 34, 113–121.
Chen, Y.L.L., Chen, H.Y., Tuo, S.H., Ohki, K., 2008. Seasonal dynamics of new production from *Trichodesmium* N_2 fixation and nitrate uptake in the upstream Kuroshio and South China Sea. Limnol. Oceanogr. 53, 1705–1721.
Chen, Y.L.L., Tuo, S.H., Chen, H.Y., 2011. Co-occurrence and transfer of fixed nitrogen from *Trichodesmium* spp. to diatoms in the low-latitude Kuroshio Current in the NW Pacific. Mar. Ecol. Prog. Ser. 421, 25–38.
Dai, M.H., Cao, Z.M., Guo, X.H., Zhai, W.D., Liu, Z.Y., Yin, Z.Q., Xu, Y.P., Gan, J.P., Hu, J.Y., Du, C.J., 2013. Why are some marginal seas sources of atmospheric CO_2? Geophys. Res. Lett. 40, 2154–2158.
Dong, W., Zheng, J., Guo, Q.J., Yamada, M., Pan, S.M., 2010. Characterization of plutonium in deep-sea sediments of the Sulu and South China Sea. J. Environ. Radioact. 101, 622–629.
Duce, R.A., Liss, P.S., Merrill, J.T., Atlas, E.L., Buat-Menard, P., Hicks, B.B., Miller, J.M., Prospero, J.M., Arimoto, R., Church, T.M., Ellis, W., Galloway, J.N., Hansen, L., Jickells, T.D., Knap, A.H., Reinhardt, K.H., Schneider, B., Soudine, A., Tokos, J.J., Tsunogai, S., Wollast, R., Zhou, M., 1991. The atmospheric input of trace species to the world ocean. Glob. Biogeochem. Cycles 5, 193–259.
Giambelluca, T.W., Chen, Q., Frazier, A.G., Price, J.P., Chen, Y.L., Chu, P.S., Eischeid, J.K., Delparte, D.M., 2013. Online rainfall atlas of Hawai'i. Bull. Am. Meteorol. Soc. https://doi.org/10.1175/BAMS-D-11-00228.1.
Giardina, M., Buffa, P., 2018. A new approach for modeling dry deposition velocity of particles. Atmos. Environ. 180, 11–22.
Hain, K., Faestermann, T., Fimiani, L., Golser, R., Gomez-Guzman, J.M., Korschinek, G., Kortmann, F., von Gostomski, C.L., Ludwig, P., Steier, P., Tazoe, H., Yamada, M., 2017. Plutonium isotopes ($^{239-241}Pu$) dissolved in Pacific Ocean waters detected by Accelerator Mass Spectrometry: no effects of the Fukushima accident observed. Environ. Sci. Technol. 51, 2031–2037.
Han, A.Q., Dai, M.H., Kao, S.J., Gan, J.P., Li, Q., Wang, L.F., Zhai, W.D., Wang, L., 2012. Nutrient dynamics and biological consumption in a large continental shelf system under the influence of both a river plume and coastal upwelling. Limnol. Oceanogr. 57, 486–502.
Hansell, D.A., Carlson, C.A., Suzuki, Y., 2002. Dissolved organic carbon export with North Pacific Intermediate Water formation. Glob. Biogeochem. Cycles 16, 1007. https://doi.org/10.1029/2000GB001361.
Hirose, K., Aoyama, M., 2003a. Analysis of ^{137}Cs and $^{239,240}Pu$ concentrations in surface waters of the Pacific Ocean. Deep-Sea Res. II 50, 2675–2700.
Hirose, K., Aoyama, M., 2003b. Present background levels of surface ^{137}Cs and $^{239,240}Pu$ concentrations in the Pacific. J. Environ. Radioact. 69, 53–60.
Hirose, K., Aoyama, M., Katsuragi, Y., Sugiyama, Y., 1987. Annual deposition of Sr-90, Cs-137 and Pu-239,240 from the 1961-1980 nuclear explosions: a simple model. J. Meteorol. Soc. Jpn. 65, 259–277.
Hirose, K., Amano, H., Baxter, M.S., Chaykovskaya, E., Chumichev, V.B., Hong, G.H., Isogai, K., Kim, C.K., Kim, S.H., Miyao, T., Morimoto, T., Nikitin, A., Oda, K., Pettersson, H.B.L., Povinec, P.P., Seto, Y., Tkalin, A., Togawa, O., Veletova, N.K., 1999. Anthropogenic radionuclides in seawater in the East Sea/Japan Sea: results of the first-stage Japanese-Korean-Russian expedition. J. Environ. Radioact. 43, 1–13.
Hirose, K., Aoyama, M., Miyao, T., Igarashi, Y., 2001. Plutonium in sea waters of the western North Pacific. J. Radioanal. Nucl. Chem. 248, 771–776.
Hirose, K., Miyao, T., Aoyama, M., Igarashi, Y., 2002. Plutonium isotopes in the sea of Japan. J. Radioanal. Nucl. Chem. 252, 293–299.
Hirose, K., Igarashi, Y., Aoyama, M., Kim, C.K., Kim, C.S., Chang, B.W., 2003. Recent trends of plutonium fallout observed in Japan: plutonium as a proxy for desertification. J. Environ. Monit. 5, 1–7.
Hirose, K., Aoyama, M., Kim, C.S., Kim, C.K., Povinec, P.P., 2006. Plutonium isotopes in seawater of the North Pacific: effects of close-in fallout. Radioact. Environ. 8, 67–82.
Honda, M.C., Aono, T., Aoyama, M., Hamajima, Y., Kawakami, H., Kitamaura, M., Masumoto, Y., Miyazawa, Y., Takigawa, M., Saino, T., 2012. Dispersion of artificial caesium-134 and -137 in the western North Pacific one month after the Fukushima

accident. Geochem. J. 46, e1–e9.
Joseph, A.B., Gustafson, P.F., Russell, I.R., Schuert, E.A., Volchok, H.L., Tamplin, A., 1971. Sources of radioactivity and their characteristics. In: Radioactivity in the Marine Environment. National Academy Sciences, Washington, pp. 6–41.
Kaeriyama, H., Shimizu, Y., Ambe, D., Masujima, M., Shigenobu, Y., Fujimoto, K., Ono, T., Nishiuchi, K., Taneda, T., Kurogi, H., Setou, T., Sugisaki, H., Ichikawa, T., Hidaka, K., Hirose, Y., Kusaka, A., Kodama, T., Kuriyama, M., Morita, H., Nakata, K., Morinaga, K., Morita, T., Watanabe, T., 2014. Southwest intrusion of ^{134}Cs and ^{137}Cs derived from the Fukushima Dai-ichi Nuclear Power Plant accident in the Western North Pacific. Environ. Sci. Technol. 48, 3120–3127.
Kanda, J., 2013. Continuing ^{137}Cs release to the sea from the Fukushima Dai-ichi Nuclear Power Plant through 2012. Biogeosciences 10, 6107–6113.
Kang, D.J., Chung, C.S., Kim, S.H., Kim, K.R., Hong, G.H., 1997. Distribution of ^{137}Cs and ^{239,240}Pu in the surface waters of the East Sea (Sea of Japan). Mar. Pollut. Bull. 35, 305–312.
Kelley, J.M., Bond, L.A., Beasley, T.M., 1999. Global distribution of Pu isotopes and ^{237}Np. Sci. Total Environ. 237–238, 483–500.
Kim, C.K., Kim, C.S., Chang, B.U., Choi, S.W., Chung, C.S., Hong, G.H., Hirose, K., Igarashi, Y., 2004. Plutonium isotopes in seas around the Korean Peninsula. Sci. Total Environ. 318, 197–209.
Kinoshita, N., Sumi, T., Takimoto, K., Nagaoka, M., Yokoyama, A., Nakanishi, T., 2011. Anthropogenic Pu distribution in Tropical East Pacific. Sci. Total Environ. 409, 1889–1899.
Kitajima, S., Furuya, K., Hashihama, F., Takeda, S., 2009. Latitudinal distribution of diazotrophs and their nitrogen fixation in the tropical and subtropical western North Pacific. Limnol. Oceanogr. 54, 537–547.
Koide, M., Bertine, K.K., Chow, T.J., Goldberg, E.D., 1985. The ^{240}Pu/^{239}Pu ratio, a potential geochronometer. Earth Planet. Sci. Lett. 72, 1–8.
Krey, P.W., 1976. Remote Pu contamination and total inventories from Rocky Flats. Health Phys. 30, 209–214.
Krey, P.W., Hardy, E.P., Pachucki, C., Rourke, F., Coluzza, J., Benson, W.K, 1976. Mass isotopic composition of global fallout plutonium in soil, Transuranium Nuclides in the Environment (Proceedings Series). IAEA, Vienna, pp. 671–678.
Kumamoto, Y., Aoyama, M., Hamajima, Y., Aono, T., Kouketsu, S., Murata, A., Kawano, T., 2014. Southward spreading of the Fukushima-derived radiocesium across the Kuroshio extension in the North Pacific. Sci. Rep. 4, 4276. https://doi.org/10.1038/srep04276.
Lee, S.Y., Huh, C.A., Su, C.C., You, C.F., 2004. Sedimentation in the Southern Okinawa Trough: enhanced particle scavenging and teleconnection between the Equatorial Pacific and western Pacific margins. Deep-Sea Res. I 51, 1769–1780.
Lettner, H., Bossew, P., Hubmer, A.K., 2000. Spatial variability of fallout caesium-137 in Austrian alpine regions. J. Environ. Radioact. 47, 71–82.
Liu, Z.Y., Zheng, J., Pan, S.M., Dong, W., Yamada, M., Aono, T., Guo, Q.J., 2011. Pu and ^{137}Cs in the Yangtze River Estuary sediments: distribution and source identification. Environ. Sci. Technol. 45, 1805–1811.
McMahon, T.A., Denison, P.J., 1979. Empirical atmospheric deposition parameters-a survey. Atmos. Environ. 13, 571–585.
METI (Ministry of Economy, Trade and Industry, Japan), 2013. http://www.meti.go.jp/earthquake/nuclear/pdf/120924/120924_01jj.pdf.
Mocak, J., Bond, A.M., Mitchell, S., Scollary, G., 1997. A statistical overview of standard (IUPAC and ACS) and new procedures for determining the limits of detection and quantification: application to voltammetric and stripping techniques. Pure Appl. Chem. 69, 297–328.
Morino, Y., Ohara, T., Nishizawa, M., 2011. Atmospheric behavior, deposition, and budget of radioactive materials from the Fukushima Daiichi nuclear power plant in March 2011. Geophys. Res. Lett. 38, L00G11. https://doi.org/10.1029/2011GL048689.
Muramatsu, Y., Hamilton, T., Uchida, S., Tagami, K., Yoshida, S., Robison, W., 2001. Measurement of ^{240}Pu/^{239}Pu isotopic rations in the soil from the Marshall Islands using ICP-MS. Sci. Total Environ. 278, 151–159.
Nakajima, K., 1973. Suspended Particulate Matter in the Western North Pacific Ocean. Hokkaido University, Sapporo, pp. 43.
Norisuye, K., Okamura, K., Sohrin, Y., Hasegawa, H., Nakanishi, T., 2006. Large volume preconcentration and purification for determining the ^{240}Pu/^{239}Pu isotopic ratio and ^{238}Pu/$^{239+240}$Pu alpha-activity ratio in seawater. J. Radioanal. Nucl. Chem. 267, 183–193.
Oikawa, S., Watabe, T., Takata, H., 2015. Distributions of Pu isotopes in seawater and bottom sediments in the coast of the Japanese archipelago before and soon after the Fukushima Dai-ichi nuclear power station accident. J. Environ. Radioact. 142, 113–123.
Oka, E., 2009. Seasonal and interannual variation of North Pacific Subtropical Mode Water in 2003–2006. J. Oceanogr. 65, 151–164.
Povinec, P.P., Hirose, K., Honda, T., Ito, T., Scott, E.M., Tagawa, O., 2004. Spatial distribution of ^{3}H, ^{90}Sr, ^{137}Cs and ^{239,240}Pu in surface waters of the Pacific and Indian Oceans-GLOMARD database. J. Environ. Radioact. 76, 113–137.
Povinec, P.P., Aarkrog, A., Buesseler, K.O., Delfanti, R., Hirose, K., Hong, G.H., Ito, T., Livingston, H.D., Nies, H., Noshkin, V.E., Shima, S., Togawa, O., 2005. ^{90}Sr, ^{137}Cs and ^{239,240}Pu concentration surface water time series in the Pacific and Indian Oceans-WOMARS results. J. Environ. Radioact. 81, 63–87.
Qu, T.D., Lukas, R., 2003. The bifurcation of the North Equatorial Current in the Pacific. J. Phys. Oceanogr. 33, 5–18.
Sakaguchi, A., Kadokura, A., Steier, P., Tanaka, K., Takahashi, Y., Chiga, H., Matsushima, A., Nakashima, S., Onda, Y., 2012. Isotopic determination of U, Pu and Cs in environmental waters following the Fukushima Daiichi Nuclear Power Plant accident. Geochem. J. 46, 355–360.
Sakaguchi, A., Steier, P., Takahashi, Y., Yamamoto, M., 2014. Isotopic compositions of ^{236}U and Pu isotopes in "Black substances" collected from roadsides in Fukushima prefecture: fallout from the Fukushima Dai-ichi nuclear power plant accident. Environ. Sci. Technol. 48, 3691–3697.
Schneider, S., Walther, C., Bister, S., Schauer, V., Christl, M., Synal, H.A., Shozugawa, K., Steinhauser, G., 2013. Plutonium release from Fukushima Daiichi fosters the need for more detailed investigations. Sci. Rep. 3, 2988. https://doi.org/10.1038/srep02988.
Shinonaga, T., Steier, P., Lagos, M., Ohkura, T., 2014. Airborne plutonium and non-natural uranium from the Fukushima DNPP found at 120 km distance a few days after reactor hydrogen explosions. Environ. Sci. Technol. 48, 3808–3814.
Shiozaki, T., Furyua, K., Kodama, T., Kitajima, S., Takeda, S., Takemura, T., Kanda, J., 2010. New estimation of N_2 fixation in the western and central Pacific Ocean and its marginal seas. Glob. Biogeochem. Cycles 24, GB1015. https://doi.org/10.1029/2009GB003620.
Suga, T., Hanawa, K., 1990. The mixed layer climatology in the northwestern part of the North Pacific subtropical gyre and the formation area of Subtropical Mode Water. J. Mar. Res. 48, 543–566.
Suga, T., Hanawa, K., 1995. The subtropical mode water circulation in the North Pacific. J. Phys. Oceanogr. 25, 958–970.
Suga, T., Takei, Y., Hanawa, K., 1997. Thermostad distribution in the North Pacific subtropical gyre: the central mode water and the subtropical mode water. J. Phys. Oceanogr. 27, 140–153.
Talley, L.D., 1997. North Pacific Intermediate Water transports in the mixed water region. J. Phys. Oceanogr. 27, 1795–1803.
Toole, J.M., Millard, R.C., Wang, Z., Pu, S., 1990. Observations of the Pacific North Equatorial current bifurcation at the Philippine coast. J. Phys. Oceanogr. 20, 307–318.
Tsumune, D., Aoyama, M., Hirose, K., 2003. Numerical simulation of ^{137}Cs and ^{239,240}Pu concentrations by an ocean general circulation model. J. Environ. Radioact. 69, 61–84.
Wang, Z.L., Yamada, M., 2005. Plutonium activities and ^{240}Pu/^{239}Pu atom ratios in sediment cores from the East China Sea and Okinawa Trough: sources and inventories. Earth Planet. Sci. Lett. 233, 441–453.
Wang, G., Xie, S.P., Qu, T., Huang, R.X., 2011. Deep South China Sea circulation. Geophys. Res. Lett. 38, L05601. https://doi.org/10.1029/2010GL046626.
Weimer, W.C., Langford, J.C., 1978. Iron-55 and stable iron in oceanic aerosols: forms and availability. Atmos. Environ. 12, 1201–1205.
Wu, J.W., Zheng, J., Dai, M.H., Huh, C.A., Chen, W.F., Tagami, K., Uchida, S., 2014. Isotopic composition and distribution of plutonium in northern South China Sea sediments revealed continuous release and transport of Pu from the Marshall Islands. Environ. Sci. Technol. 48, 3136–3144.
Wu, J.W., Dai, M.H., Xu, Y., Zheng, J., 2018. Sources and accumulation of plutonium in a large Western Pacific marginal sea: the South China Sea. Sci. Total Environ. 610–611, 200–211.
Yamada, M., Zheng, J., 2008. Determination of ^{240}Pu/^{239}Pu atom ratio in coastal surface seawaters from the western North Pacific Ocean and Japan Sea. Appl. Radiat. Isot. 66, 103–107.
Yamada, M., Zheng, J., 2011. Determination of ^{240}Pu/^{239}Pu atom ratio in seawaters from the East China Sea. Radiat. Prot. Dosim. 146, 311–313.
Yamada, M., Zheng, J., Wang, Z.L., 2006. ^{137}Cs, $^{239+240}$Pu and ^{240}Pu/^{239}Pu atom ratios in the surface waters of the Western North Pacific Ocean, Eastern Indian Ocean and their adjacent seas. Sci. Total Environ. 366, 242–252.
Yamada, M., Zheng, J., Wang, Z.L., 2007. ^{240}Pu/^{239}Pu atom ratios in seawater from Sagami Bay, Western Northwest Pacific Ocean: sources and scavenging. J. Environ. Radioact. 98, 274–284.
Yamamoto, M., Sakaguchi, A., Ochiai, S., Takada, T., Hamataka, K., Murakami, T., Nagao, S., 2014. Isotopic Pu, Am and Cm signatures in environmental samples contaminated by the Fukushima Dai-ichi nuclear power plant accident. J. Environ. Radioact. 132, 31–46.
Yasuda, I., Okuda, K., Shimizu, Y., 1996. Distribution and modification of North Pacific Intermediate Water in the Kuroshio-Oyashio interfrontal zone. J. Phys. Oceanogr. 26, 448–465.
Yoshida, N., Kanda, J., 2012. Tracking the Fukushima radionuclides. Science 336, 1115–1116.
Zhang, D., Johns, W.E., Lee, T.N., 2002. The seasonal cycle of meridional heat transport at 24° N in the North Pacific and in the global ocean. J. Geophys. Res. Oceans 107, C7. https://doi.org/10.1029/2001JC001011.
Zheng, J., Yamada, M., 2004. Sediment core record of global fallout and Bikini close-in fallout Pu in Sagami Bay, western Northwest Pacific margin. Environ. Sci. Technol. 38, 3498–3504.
Zheng, J., Yamada, M., 2005. Vertical distributions of $^{239+240}$Pu activities and ^{240}Pu/^{239}Pu atom ratios in sediment cores: implications for the sources of Pu in the Japan Sea. Sci. Total Environ. 340, 199–211.
Zheng, J., Yamada, M., 2006. Plutonium isotopes in settling particles: transport and scavenging of Pu in the western Northwest Pacific. Environ. Sci. Technol. 40, 4103–4108.
Zheng, J., Tagami, K., Watanabe, Y., Uchida, S., Aono, T., Ishii, N., Yoshida, S., Kubota, Y., Fuma, S., Ihara, S., 2012. Isotopic evidence of plutonium release into the environment from the Fukushima DNPP accident. Sci. Rep. 2, 304. https://doi.org/10.1038/srep00304.
Zheng, J., Tagami, K., Uchida, S., 2013. Release of plutonium isotopes into the environment from the Fukushima Daiichi nuclear power plant accident: what is known and what needs to be known. Environ. Sci. Technol. 47, 9584–9595.